

Jordan Journal of Physics

ARTICLE

Crystallization Behavior of $\text{Se}_{85}\text{Cd}_8\text{Zn}_7$ Chalcogenide Glass

Omar A. Lafi

Department of Physics, Faculty of Science, Al-Balqa Applied University, Al-Salt-19117, Jordan.

Received on: 12/4/2016;

Accepted on: 16/8/2016

Abstract: Ternary $\text{Se}_{85}\text{Cd}_8\text{Zn}_7$ chalcogenide glass was prepared by melt quenching technique. Experimental measurements by differential scanning calorimeter (DSC) are used for studying crystallization behavior of this glass under non-isothermal conditions. DSC curves show well defined endothermic and exothermic peaks at glass transition (T_g) and crystallization peak (T_c) temperatures. The T_c dependence on the heating rate (β) is utilized in the determination of the crystallization activation energy (E_c) and the Avrami exponent (n). These crystallization parameters were deduced using Kissinger, Takhor, Augis-Bennett and Ozawa-Matusita methods. The theoretical derivations of these methods were discussed in this work. The resulting values of E_c obtained from the different methods agree good with each other and the obtained value of Avrami exponent ($n = 0.87$) indicated that the crystal growth in $\text{Se}_{85}\text{Cd}_8\text{Zn}_7$ glass occurs in one dimension.

Keywords: Chalcogenide glasses; Differential scanning calorimeter (DSC); Crystallization activation energy; Dimensionality of crystal growth.

Introduction

Over the past few decades, the unique properties of chalcogenide glasses (including selenium, tellurium, sulfur and their compounds) have encouraged researchers to understand the important processes proceeding in these materials for further development and search for new application possibilities. Crystallization (the process when glass in a metastable state is heated high enough for its structure to be able to "de-freeze" and transform into a more thermodynamically stable crystalline state) is one of the important processes in the field of chalcogenide glass. The most promising properties of chalcogenide glass, in its amorphous state, have been found to deteriorate drastically during crystallization. Therefore, studying and then understanding the crystallization mechanism to impede or control crystallization is a prerequisite for most of the applications, as stability against crystallization determines effective working limits [1]. Several attempts [2-8] are still made nowadays to

investigate the crystallization kinetics of binary or multi-component chalcogenide systems.

Studying the crystallization kinetics can be carried out by two basic methods: isothermal and non-isothermal. In the isothermal method, the sample is brought quickly to a fixed temperature above the glass transition temperature (T_g) and the heat evolved during the crystallization process at this constant temperature is recorded as a function of time. In the non-isothermal method, the sample is heated at a fixed rate (β) and the heat evolved is recorded as a function of temperature. Non-isothermal measurements using a constant heating rate are more commonly used because of their several advantages, such as the quick performance and the rapid information they provide on the transformation temperatures, like glass transition temperature (T_g) and crystallization temperature (T_c) [9]. Differential scanning calorimetry (DSC) is an extremely popular method for studying non-isothermal transformation kinetics. The appeal of this

method is simplicity and flexibility in the selection of heating (cooling) rates. Crystallization kinetics (under non-isothermal conditions) can always be analyzed by the determination of crystallization activation energy (E_c) and the dimensionality of crystal growth (m).

Zinc selenide (ZnSe) has unique physical properties, such as wide optical energy band gap, high refractive index and low optical absorption in the visible and infrared spectral regions. Therefore, it has several potential applications, such as blue light emitting diodes, photodiodes, thin film transistors and Cr-doped ZnSe laser [10]. On the other hand, cadmium selenide (CdSe) is widely preferred in fabrication of solar cells, photodetectors, light emitting diodes and other opto-electronic devices owing to its high photosensitive behavior [11]. According to the author's knowledge, no work has been conducted to study crystallization behavior of Se-based ternary chalcogenide glasses containing both Cd and Zn as dopant materials. Therefore, this work aims to investigate, using differential scanning calorimeter, the crystallization kinetics of the ternary $\text{Se}_{85}\text{Cd}_8\text{Zn}_7$ chalcogenide glass under non-isothermal conditions. The dependence of the crystallization peak temperature (T_c) on heating rate (β) will be used for the calculation of the crystallization activation energy of $\text{Se}_{85}\text{Cd}_8\text{Zn}_7$ glass, using different theoretical methods which will be discussed in this work. This further will be used for determining the dimensionality of crystal growth.

Theoretical Basis

The general Johnson-Mehl-Avrami (JMA) equation for solid state transformation can be used to describe the kinetics of crystallization for many amorphous materials [12]. This equation is based upon the following assumptions [13]: (1) the system is in a quasi-equilibrium state and the rate at which the atoms leave the initial state is so small that the energy distribution of the initial state is undisturbed, (2) the rate is not diffusion limited and (3) the crystallization mechanism is of a nucleation and growth type, (4) nucleation is spatially random and (5) the process takes place under isothermal conditions. JMA equation describes the time evolution of the overall crystallinity. According to these assumptions, the fraction X of the material that crystallized after a time t can be written as [14-17]:

$$X = 1 - \exp[-(Kt)^n]; \quad (1)$$

where n is the Avrami exponent that reflects the details of crystal growth. K is the effective overall reaction rate (including both nucleation and growth), which is actually a measure of the rate of crystallization and usually assigned Arrhenius temperature dependence:

$$K = K_0 \exp\left(-\frac{E_c}{RT}\right). \quad (2)$$

Here, K_0 , a frequency factor, indicates the number of attempts to overcome the energy barrier and E_c is the activation energy for crystallization. Based on JMA equation, different authors [18-23] have developed different methods to study the crystallization process by calculating the crystallization activation energy E_c and the order of crystallization n .

Kissinger Method

This method is most widely used in analyzing crystallization data obtained from DSC measurements. In non-isothermal DSC experiments, at a constant heating rate β ($= dT/dt$), the sample temperature T changes linearly with time according to the relation:

$$T = T_i + \beta t; \quad (3)$$

where T_i is the temperature at the beginning of the experiment which is usually equal to room temperature.

The derivative of K with respect to time can be obtained from Eqs. (2) and (3) as follows:

$$\frac{dK}{dt} = \left(\frac{dK}{dT}\right)\left(\frac{dT}{dt}\right) = \left(\frac{\beta E_c}{RT^2}\right)K. \quad (4)$$

Eq. (1) can be differentiated as:

$$\frac{dX}{dt} = n(Kt)^{n-1}[K + (dK/dt)t](1-X). \quad (5)$$

Substituting Eq. (4) in Eq. (5), we get:

$$\frac{dX}{dt} = nK^n t^{n-1}[1 + \alpha t](1-X); \quad (6)$$

where $\alpha = (\beta E_c / RT^2)$.

According to Kissinger [18], the term αt can be neglected in comparison to unity ($(E_c / RT^2) \ll 1$), and then Eq. (6) becomes:

$$\frac{dX}{dt} = (1-X)nK^n t^{n-1} . \quad (7)$$

If we express t in terms of X from Eq. (1), the crystallization rate dX/dt can be written as:

$$\frac{dX}{dt} = AnK (1-X) ; \quad (8)$$

where $A = [-\ln(1-X)]^{(n-1)/n}$.

Using Eqs. (4) and (8), the second derivative $d^2X/dt^2 = 0$ at the crystallization peak temperature T_c , then Kissinger showed that [18]:

$$\ln\left(\frac{\beta}{T_c^2}\right) = -\frac{E_c}{RT_c} + C . \quad (9)$$

This equation is used to calculate the activation energy of crystallization by plotting $\ln(\beta/T_c^2)$ versus $1/T_c$.

Takhor Method

Takhor [22] suggested a method which makes the assumption of ignoring the time dependence of K in the second differentiation. Assuming that $K \neq K(t)$, the differentiation of Eq. (7) with respect to time yields:

$$\frac{d^2X}{dt^2} = nK^n t^{n-2} [(n-1) - nK^n t^n] . \quad (10)$$

The maximum rate of crystallization occurs at peak crystallization temperature T_c and time t_p , where $d^2X/dt^2 = 0$, and if we convert the value of t_p to temperature T_c from Eq. (3), we get [24]:

$$n \ln \beta - n \ln(T_c - T_i) = \ln \frac{nK_0}{n-1} - \frac{nE_c}{RT_c} . \quad (11)$$

With the assumption that $n \ln(T_c - T_i)$ is a function which changes more slowly with heating rate than $1/T_c$, we get:

$$\frac{d \ln \beta}{d(1/T_c)} = -\frac{E_c}{R} . \quad (12)$$

On this basis, the slope of $\ln \beta$ versus $1/T_c$ should yield the crystallization activation energy E_c .

Augis-Bennett Method

The standard method of Augis and Bennet gives more exact results for deducing the crystallization parameters when the

crystallization appears at a temperature much higher than the initial one ($T_c \gg T_i$). Based on substituting $u = KT$ in Eq. (6), we get:

$$\frac{dX}{dt} = X' = nKu^{n-1}[1+\alpha t](1-X) . \quad (13)$$

Since $u' = K'T + K$ and using Eq. (4), one obtains:

$$X' = nu'u^{n-1}(1-X) \quad (14)$$

and

$$X'' = [u''u - (u')^2(nu^n - n + 1)]nu^{n-2}(1-X) . \quad (15)$$

$X'' = d^2X/dt^2 = 0$ at crystallization peak temperature T_c , where the maximum rate of crystallization occurs. This gives:

$$u''u - (u')^2(nu^n - n + 1) = 0 . \quad (16)$$

From substituting $u = KT$ and $T = T_i + \beta t$ in JMA equation, one can find that:

$$u' = \frac{u}{t} + \alpha u = u\left(\frac{1}{t} + \alpha\right) ; \quad (17)$$

$$u'' = u'\left(\frac{1}{t} + \alpha\right) - \frac{u}{t^2} = u\left[\left(\frac{1}{t} + \alpha\right)^2 - \frac{1}{t^2}\right] - \frac{2\alpha u}{t} . \quad (18)$$

The last term in Eq. (18) above was omitted in the original derivation of Augis and Bennet [21], and this equation can be simplified as:

$$u'' = u\alpha^2 . \quad (19)$$

Substituting for u' and u'' from Eqs. (17) and (19) into Eq. (16) gives:

$$nu^n - n + 1 = \left(\frac{\alpha t}{1 + \alpha t}\right)^2 . \quad (20)$$

Eq. (20) is discussed in light of the possible values of αt and the relation between the temperatures T and T_i . The term αt can be expressed by substituting the value of $\beta = \alpha RT^2/E_c$ in Eq. (3) as [25]:

$$\alpha t = \frac{E_c}{RT} \left(1 - \frac{T_i}{T}\right) . \quad (21)$$

When $at \ll 1$ and the temperature T is slightly higher than T_i ($(E_c / RT) \ll 1$), we can neglect the term at and Eq. (20) leads directly to Kissinger equation. Besides, when $at \gg 1$ and $T \gg T_i$, then $(E_c / RT) \gg 1$, the right hand side of Eq. (20) approaches unity and this gives $u^n = 1$ and hence $u = 1$. Therefore, we can write:

$$u = (Kt)_p = K_0 \exp\left(\frac{E_c}{RT_c}\right) \left[\frac{T_c - T_i}{\beta}\right] \cong 1. \quad (22)$$

This equation can be written in logarithmic form as:

$$\ln\left(\frac{\beta}{T_c - T_i}\right) = -\frac{E_c}{RT_c} + \ln K_0. \quad (23)$$

Finally, in the case of $(T_c \gg T_i)$, this equation can be approximated as:

$$\ln\left(\frac{\beta}{T_c}\right) = -\frac{E_c}{RT_c} + \ln K_0. \quad (24)$$

The activation energy E_c can be evaluated from the slope of the plot of $\ln(\beta / T_c)$ as a function of $1/T_c$.

Determination of Avrami Exponent (n)

Avrami exponent (n) can be simply found from the original JMA equation. Substituting the value of t from Eq. (3) in the JMA equation (Eq. (1)) and rearranging we get:

$$1 - X = \exp\left[-\left(\frac{K(T - T_i)}{\beta}\right)^n\right]. \quad (25)$$

By taking the double logarithm of the above equation, one can find that:

$$\frac{d \ln[-\ln(1 - X)]}{d \ln \beta} = -n. \quad (26)$$

This relation was derived individually by Ozawa [19, 20] and Matusita *et al.* [21]. According to this relation, Avrami exponent (n) can be evaluated by plotting $\ln[-\ln(1 - X)]$ as a function of $\ln \beta$ at a constant temperature T . The fraction X crystallized at any temperature T is given as $X = A_T/A$, where A is the total area of the exothermic peak between the temperature T_1 where crystallization just begins and the temperature T_2 where crystallization is completed and A_T is the area between T_1 and a

given temperature T as shown in Fig. 1. For as-quenched glass containing no preexisting nuclei, the dimensionality of crystal growth (m) is equal to $(n - 1)$ and m will be 1 if n is less than 2, whereas for a glass containing a sufficiently large number of nuclei, which might occur due to annealing of the as-quenched glass, $m = n$. In this work, as-quenched samples are studied, then the value of m is taken as $m = n - 1$ [23].

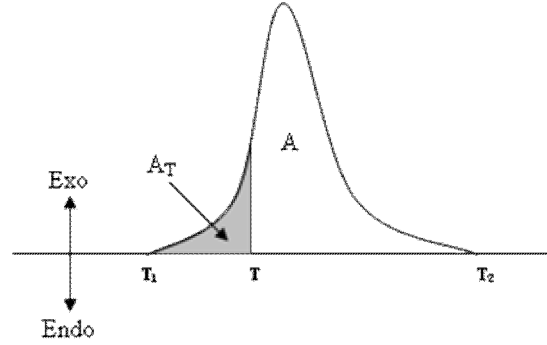


FIG. 1. A typical DSC exothermic peak indicating the estimation of the fraction X crystallized at any temperature T .

Material Preparation and Experimental Technique

$\text{Se}_{85}\text{Cd}_8\text{Zn}_7$ glass was prepared by melt quenching technique. High purity (5N) Se, Cd and Zn in appropriate atomic weight percentage (at. wt %) proportions were weighed into a quartz ampoule and sealed at a vacuum of 10^{-5} Torr. The ampoules were then heated at 900 °C for about 15 h with continuous rotation to facilitate the homogenization of the sample. The molten sample was rapidly quenched in ice-cooled water to produce a glassy state. The ingot of the so-produced glassy sample was taken out of the ampoule by breaking the ampoule and then grinding the sample gently in a mortar and pestle to obtain a powder form. About 10 mg of the powder samples were capsulated in aluminum pan and subjected to the differential scanning calorimeter (NETZSCH DSC 200 F3) at five heating rates (5, 10, 15, 20 and 25 K/min) in the temperature range from room temperature to about 750K. The temperature accuracy of this equipment is $\pm 0.1\text{K}$. The DSC equipment is calibrated prior to measurements, using high purity standard Pb, Sn and In with well-known melting points. The operation of a differential scanning calorimeter is based on the measurement of the thermal response of an unknown specimen as compared with a standard when the two are uniformly heated. A typical

differential scanning calorimeter consists of two sealed pans; a sample pan and an empty reference pan. These pans are often covered by or composed of aluminum, which acts as a radiation shield. The two pans are uniformly heated, or cooled, while the heat flow difference between the two is monitored.

Results and Discussion

Typical DSC curves of $\text{Se}_{85}\text{Cd}_8\text{Zn}_7$ glass at five different heating rates (5, 10, 15, 20 and 25 K/min) are shown in Fig.2. Two characteristic phenomena are evident in these DSC curves in the temperature range of investigation. The first one (endothermic peak) corresponds to the glass transition region and is represented by the glass transition temperature (T_g). The second one (exothermic peak) corresponds to the crystallization region and is represented by the crystallization peak temperature (T_c). At this temperature (T_c), the crystallization rate reaches two-thirds of its value [4]. The appearance of

single glass transition peak and single crystallization peak confirms that the glassy sample under investigation is homogeneous. Both T_g and T_c have been defined [1, 9] as the temperatures which correspond to the intersection of two linear portions adjoining the transition elbow of the DSC traces in the endothermic and exothermic directions, respectively. The values of T_g and T_c at all heating rates are given in Table 1. From this table, one can notice that both T_c and T_g of the studied samples are much higher than room temperature. Thus, one can expect that the studied sample may remain stable in its amorphous and crystalline phases at room temperature. In addition, the temperature difference ($T_c - T_g$) is large. This is an advantage of the studied glass, as it is essential to prevent self-transition between the two amorphous and crystalline phases, making it attractive for optical recording applications [26].

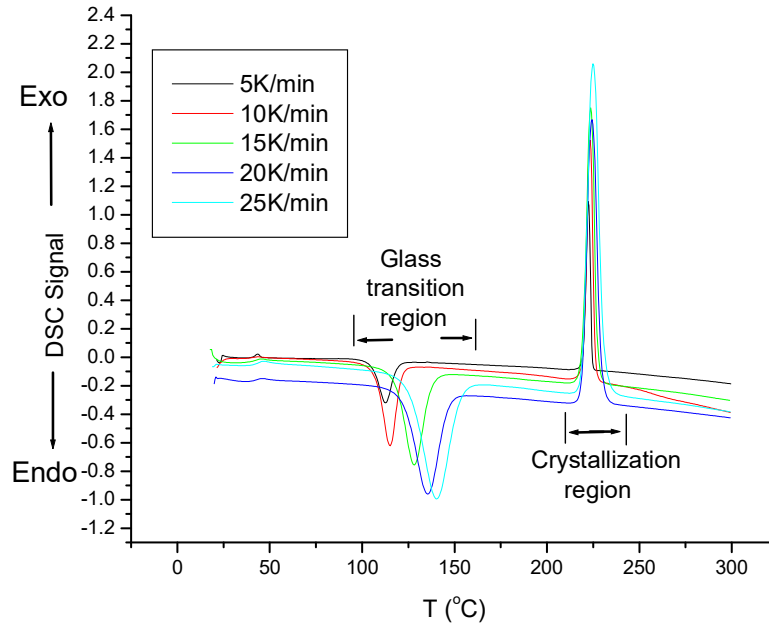


FIG. 2. Typical DSC curves for $\text{Se}_{85}\text{Cd}_8\text{Zn}_7$ glass at five different heating rates (5, 10, 15, 20 and 25 K/min).

TABLE. 1. The values of T_g and T_c of the studied glass at different heating rates

Heating rate (K/min)	T_g (K)	T_c (K)
5	377.2	495.0
10	385.7	496.2
15	390.1	496.9
20	394.0	497.4
25	396.5	497.9

The crystallization kinetics of the studied glass were analyzed by calculating the crystallization activation energy (E_c) and Avrami exponent (n) which is related to the dimensionality of crystal growth (m). These parameters were calculated from the dependence of the crystallization peak temperature (T_c) on heating rate (β) according to the theoretical methods discussed in Section 2. Firstly, according to Eq. (9), which was derived by Kissinger, the data of $\ln(\beta/T_c^2)$ versus ($10^3/T_c$) for $\text{Se}_{85}\text{Cd}_8\text{Zn}_7$ glass is fitted to linear function by least square fitting as shown in Fig. 3. From the slope of this fit, the value of the

activation energy (E_c) is obtained to be (1143 ± 24) kJ/mol. Secondly, E_c was determined using Takhor method according to Eq. (12). In this method, the activation energy is evaluated from the slope of the least square fitting of the plot of $\ln \beta$ versus ($10^3/T_c$) which is shown in Fig. 4.

The value of E_c deduced by this method is (1151 ± 24) kJ/mol. Finally, E_c was calculated using Augis and Bennett approximation method as given in Eq. (24). Fig. 5 shows the plot of $\ln(\beta/T_c)$ against ($10^3/T_c$) and from the slope of the straight line of the least square fitting of all points, the value of E_c is obtained to be (1147 ± 24) kJ/mol.

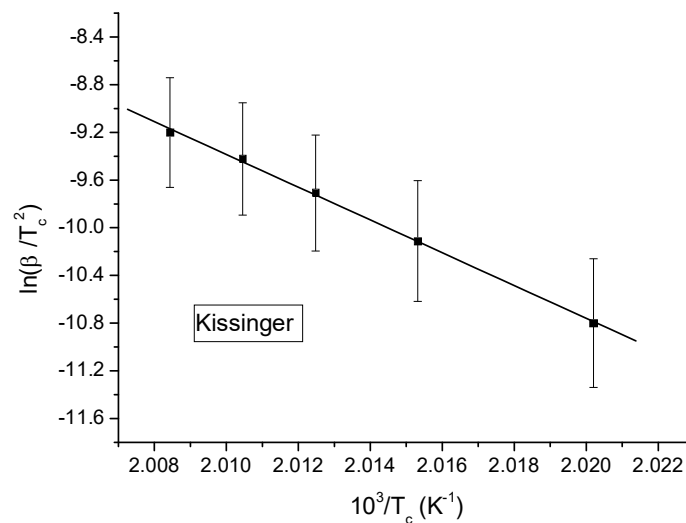


FIG. 3. Plot of $\ln(\beta/T_c^2)$ vs. ($10^3/T_c$) for $\text{Se}_{85}\text{Cd}_8\text{Zn}_7$ glass (solid line is least-square fit to Kissinger relation (Eq. 9)).

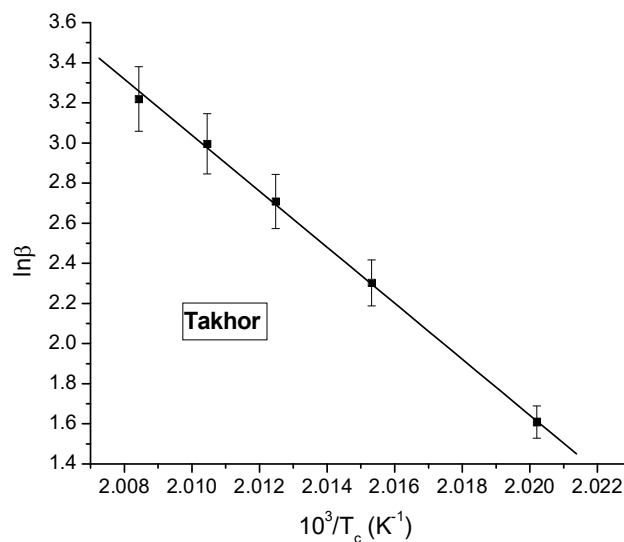


FIG. 4. Plot of $\ln \beta$ vs. ($10^3/T_c$) for $\text{Se}_{85}\text{Cd}_8\text{Zn}_7$ glass (solid line is least-square fit to Takhor relation (Eq. 12)).

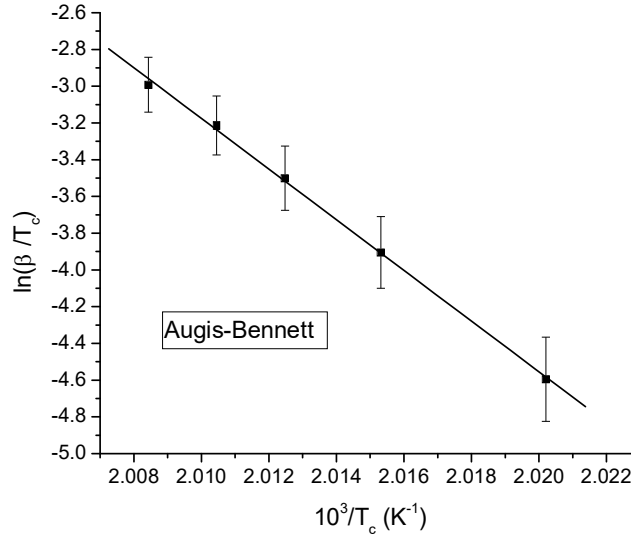


FIG. 5. Plot of $\ln(\beta/T_c)$ vs. $(10^3/T_c)$ for $\text{Se}_{85}\text{Cd}_8\text{Zn}_7$ glass (solid line is least-square fit to Augis and Bennett approximation relation (Eq. 24)).

The above E_c values, obtained from the three methods, are well consistent with each other. However, Augis and Bennet method gives more exact results for deducing E_c value when the crystallization appears often at a temperature which is much higher than the initial one $T_c \gg T_i$. It was shown [27] that this method can be applied, not only in the case $T_c \gg T_i$, but also when $T_c > T_i$; that is, when the two temperatures differ by about 10%. Besides, the crystallization activation energy is an indication of the speed of rate of crystallization which is useful to characterize the glass for optical recording and other applications [28]. It is clear that the value of E_c of $\text{Se}_{85}\text{Cd}_8\text{Zn}_7$ glass, which is required to complete the crystallization process, is higher than that of similar glasses. This could be explained on the basis of bond formation in the complex matrices.

According to Schotmiller et al. [29], in amorphous Se, about 40% of the atoms have a ring structure (Se_8) and 60% of the atoms are bonded as polymeric chains ($-\text{Se}-\text{Se}-\text{Se}-$). Strong covalent bonds exist between the atoms in the chains and rings, whereas the inter-structural forces are weak bonds of Van der Waal's type [30]. When Zn is incorporated to Se, the metallic Zn bonds dissolved in Se chains and the weaker Se-Se bonds (bond energy = 44.0 kcal/mole) are replaced by the strong Se-Zn bonds (bond energy = 64.0 kcal/mole) [31]. In addition to Se-Zn heteronuclear bonds, Zn-Zn and Se-Se homonuclear bonds are expected to exist. Further, when Cd is added to the Se-Zn

system, it forms bonds with Se (Se-Cd bond energy = 37.1 kcal/mole [9]), while the formation of Zn-Cd, Cd-Cd and Se-Zn-Cd can also exist in the same matrix. The extensive existence of heteronuclear and homonuclear bonds heavily cross-linked the ternary matrix structure and increased the steric hindrance, which play a dominant role in the glass configuration [32]. On the other hand, Pauling defined the electronegativity of an atom as its power to attract electrons to itself in the molecule [33]. When two elements of different electronegativity values combine to form an alloy, then the element of higher electronegativity attracts an electron pair more than the other elements and behaves as an anion. The other element will behave as a cation [34]. The values of electronegativity of Se, Cd and Zn are 2.4, 1.7, and 1.6, respectively. Therefore, Se behaves as an anion, while both of Zn and Cd (from the same IIB group) are considered as cations. The presence of Zn and Cd cations together can create a large number of unsaturated hydrogen-like bonds accompanied with Van der Waal's bonds, substantially increasing the structural and thermal stability of the glass [35]. This is responsible for increasing the strength or rigidity of the lattice, which increases the tendency of the glass against crystallization and consequently the crystallization activation energy.

The order of crystallization reaction (Avrami exponent) for $\text{Se}_{85}\text{Cd}_8\text{Zn}_7$ glass was obtained using the method suggested by Ozawa and

Matusita. The plot of $\ln[-\ln(1-X)]$ vs. $\ln\beta$ for $\text{Se}_{85}\text{Cd}_8\text{Zn}_7$ glass is shown in Fig. 6 at different temperatures (494K, 495K, 496K and 497K). The average value of Avrami exponent n , obtained from the slopes of the fitted straight lines in Fig.6, comes out to be 0.87. Based on this value, the crystal growth in $\text{Se}_{85}\text{Cd}_8\text{Zn}_7$ glass occurs in one dimension (or growth from surface nuclei). This value of Avrami exponent is non-integer. A non-integer value of n indicates that two crystallization mechanisms were working during the amorphous–crystalline transformation [26, 36]. Lastly, it is worth to mention that some other thermal models [37-40] used in the study of the non-isothermal crystallization mechanism

suggested that the values of n and E_c are not necessarily constant, but show variations in different stages of the transformation. The models used in this work are proposed for analyzing the non-isothermal crystallization kinetics, in the case of as-quenched glasses which contain a large number of nuclei, “site saturation”. This “site saturation” assumption is important for this process, where the crystallization rate is only defined by the temperature and shows little dependence on the thermal history, and then the variation in the values of the crystallization parameters (n and E_c) during all stages of transformation process is not expected [41].

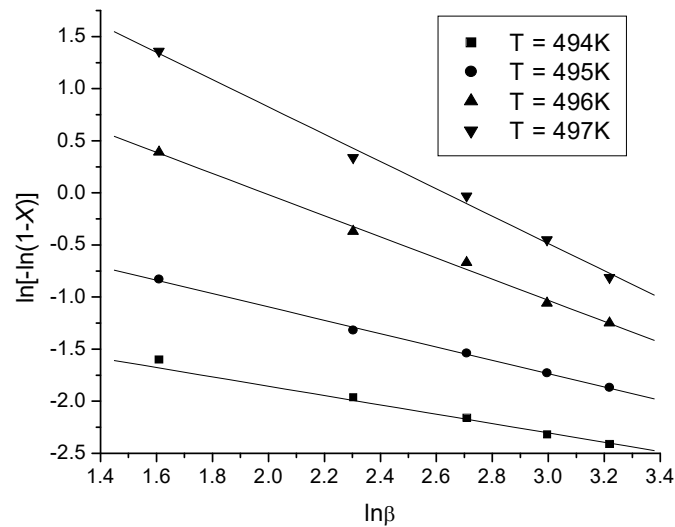


FIG. 6. Plot of $\ln[-\ln(1-X)]$ vs. $\ln\beta$ for $\text{Se}_{85}\text{Cd}_8\text{Zn}_7$ glass at different selected temperatures (solid lines are least-square fits to Ozawa-Matusita relation (Eq. 26)).

Conclusions

Crystallization kinetics for $\text{Se}_{85}\text{Cd}_8\text{Zn}_7$ glass have been investigated using differential scanning calorimeter DSC under non-isothermal conditions. The obtained data has been analyzed by several theoretical methods. The following conclusions were drawn:

1. The glassy alloy under investigation shows single glass transition region and single crystallization region, confirming the homogeneity of the glassy sample.
2. The values of E_c obtained using the three different methods; Kissinger, Takhor and Augis-Bennett, are in good agreement with each other. Thus, one can use any of these methods to deduce the activation energy of crystallization.

3. One-dimensional crystal growth occurs in $\text{Se}_{85}\text{Cd}_8\text{Zn}_7$ glass, indicated by the estimated value of Avrami exponent ($n = 0.87$).

Acknowledgment

This work has been carried out during sabbatical leave granted to the author (O.A. Lafi) from Al-Balqa Applied University during the academic year 2015/2016; therefore, it deserved great thanks. The author is also grateful to the Department of Physics at the University of Jordan for providing all facilities during this research work.

References

- [1] Imran, M.M.A., Bhandari, D. and Saxena, N.S., *J. Therm. Anal. Calorim.*, 65 (2001) 257.
- [2] Lafi, O.A., Imran, M.M.A., Abu-Shaweesh, N.I., Al-Kurdi, F.M. and Khatatbeh, I.K., *J. Phys. Chem. Solids*, 75 (2014) 790.
- [3] Lafi, O.A., Imran, M.M.A., Abdullah, M.K. and Al-Sakhel, S.A., *Thermochimica Acta*, 560 (2013) 71.
- [4] Imran, M.M.A., *Physica B*, 406 (2011) 482.
- [5] Tanwar, N. and Saraswat, V.K., *J. Non-Cryst. Solids*, 394 (2014) 1.
- [6] Xu, W., Ren, J. and Guorong, C., *J. Non-Cryst. Solids*, 398-399 (2014) 42.
- [7] Svoboda, R. and Málek, J., *J. Alloys Comp.*, 627 (2015) 287.
- [8] Štrbac, G.R., Štrbac, D.D., Lukić-Petrović, S.R. and Šiljegović, M.V., *J. Non-Cryst. Solids*, 426 (2015) 92.
- [9] Lafi, O.A., *J. Alloys Comp.*, 519 (2012) 123.
- [10] Abdel-Rahim, M.A., Hafiz, M.M., Elwhab, A. and Alwany, B., *Optics and Laser Technology*, 44 (2012) 1116.
- [11] Kalita, K.R.P., Sarma, B.K. and Das, H.L., *Bull. Mater. Sci.*, 26(6) (2003) 613.
- [12] Marseglia, E.A., *J. Non-Cryst. Solids*, 41 (1980) 31.
- [13] White, K., Crane, R.N. and Snide, J.A., *J. Non-Cryst. Solids*, 103 (1988) 210.
- [14] Johnson, W.A. and Mehl, K.F., *Trans. Amer. Inst. Mining Met. Egrs.*, 135 (1981) 315.
- [15] Avrami, M., *J. Chem. Phys.*, 7 (1939) 1103.
- [16] Avrami, M., *J. Chem. Phys.*, 8 (1940) 212.
- [17] Avrami, M., *J. Chem. Phys.*, 9 (1941) 177.
- [18] Kissinger, H.E., *J. Res. Nat. Bur. Stand.*, 57(4) (1956) 217.
- [19] Ozawa, T., *Bul. Chem. Soc., Japan*, 38 (1965) 1881.
- [20] Ozawa, T., *Polymer*, 12 (1971) 150.
- [21] Augis, J.E. and Bennet, J., *J. Therm. Anal.*, 13 (1978) 283.
- [22] Takhor, R.L., "Advance in Nucleation and Crystallization of Glasses", (American Ceramic Society, Columbus, 1972), p.253.
- [23] Matusita, T., Komatsu, T. and Yokota, R., *J. Mat. Science*, 19 (1984) 291.
- [24] Uinnon, H. and Uhlmann, D.R., *J. Non-Cryst. Solids*, 54 (1983) 253.
- [25] Kozmidis-Petrović, A.F., Štrbac, G.R. and Štrbac, D.D., *J. Non-Cryst. Solids*, 353 (2007) 2014.
- [26] Srivastava, S., Zulfequar, M., Agrahari, S.K. and Kumar, A., *Physica B*, 403 (2008) 3429.
- [27] Kozmidis-Petrović, A.F., Lukić, S.R. and Štrbac, G.R., *J. Non-Cryst. Solids*, 356 (2010) 2151.
- [28] Khan, S.A., Al-Hazmi, F.S., Faidah, A.S. and Al-Ghamdi, A.A., *Curr. Appl. Phys.*, 9 (2009) 567.
- [29] Schotmiller, J., Tabak, M., Lucovsky, G. and Ward, A., *J. Non-Cryst. Solids*, 4 (1970) 80.
- [30] Thiruvikraman, P.K., *Bull. Mater. Sci.*, 29(4) (2006) 371.
- [31] Abdel-Rahim, M.A., Hafiz, M.M., Elwhab, A. and Alwany, B., *Optics and Laser Technology*, 47 (2013) 88.
- [32] Singh, A.K., *Optik*, 124 (2012) 2187.
- [33] Pauling, L., "The Nature of the Chemical Bond", 3rd Ed. (Cornell University Press, 1960).
- [34] Shukla, R.K., Swarupt, S., Kumar, A. and Nigam, A.N., *Semicond. Sci. Technol.*, 4 (1988) 681.
- [35] Singh, A.K., *J. Alloys Comp.*, 552 (2013) 166.
- [36] Al-Heniti, S.H., *J. Alloys Comp.*, 484 (2009) 177.
- [37] Vyazovkin, S., *New J. Chem.*, 24 (2000) 913.
- [38] Vyazovkin, S., *Thermochimica Acta*, 355 (2000) 269.
- [39] Abdel-Rahim, M.A., Hafiz, M.M. and Mahmoud, A.Z., *Progress in Natural Science: Materials International*, 25 (2015) 169.
- [40] Abdelazim, N.M., Abdel-Latif, A.Y., Abu-Sehly, A.A. and Abdel-Rahim, M.A., *J. Non-Cryst. Solids*, 387 (2014) 79.
- [41] Málek, J., *Thermochimica Acta*, 355 (2000) 239.